Neuron, Vol. 35, 843–854, August 29, 2002, Copyright ©2002 by Cell Press

Testosterone Reduction Prevents Phenotypic Expression in a Transgenic Mouse Model of Spinal and Bulbar Muscular Atrophy

Masahisa Katsuno,[1,4] Hiroaki Adachi,[1,4] Akito Kume,[1] Mei Li,[1] Yuji Nakagomi,[2] Hisayoshi Niwa,[1] Chen Sang,[1] Yasushi Kobayashi,[1] Manabu Doyu,[1] and Gen Sobue[1,3]

[1]Department of Neurology
Nagoya University Graduate School of Medicine
65 Tsurumai-cho
Showa-ku, Nagoya 466-8550
Japan

[2]Laboratory of Electron Microscopy
Aichi Medical University
21 Karimata, Yazako
Nagakute-cho, Aichi 480-1195
Japan

Summary

Spinal and bulbar muscular atrophy (SBMA) is a polyglutamine disease caused by the expansion of a CAG repeat in the *androgen receptor* (*AR*) gene. We generated a transgenic mouse model carrying a full-length *AR* containing 97 CAGs. Three of the five lines showed progressive muscular atrophy and weakness as well as diffuse nuclear staining and nuclear inclusions consisting of the mutant AR. These phenotypes were markedly pronounced in male transgenic mice, and dramatically rescued by castration. Female transgenic mice showed only a few manifestations that markedly deteriorated with testosterone administration. Nuclear translocation of the mutant AR by testosterone contributed to the phenotypic difference with gender and the effects of hormonal interventions. These results suggest the therapeutic potential of hormonal intervention for SBMA.

Introduction

Spinal and bulbar muscular atrophy (SBMA) is an X-linked late-onset motor neuron disease characterized by proximal muscle atrophy, weakness, contraction fasciculations, and bulbar involvement (Kennedy et al., 1968; Sobue et al., 1989). Heterozygous female carriers are usually asymptomatic, although some express subclinical phenotypes, including high amplitude motor unit potentials on electromyography (Sobue et al., 1993; Mariotti et al., 2000). A specific treatment for SBMA has not been established. Testosterone may improve motor function in some patients, although it has no effects on the progression of SBMA (Danek et al., 1994; Goldenberg and Bradley, 1996; Neuschmid-Kaspar et al., 1996).

The molecular basis of SBMA is the expansion of a trinucleotide CAG repeat in the first exon of the *androgen receptor* (*AR*) gene, which encodes the polyglutamine (polyQ) tract (La Spada et al., 1991). Thus, SBMA was the first described member of polyQ diseases including Huntington's disease (HD), several forms of spinocerebellar ataxia, and dentatorubral and pallidoluysian atrophy (DRPLA) (Zoghbi and Orr, 2000; Paulson, 2000). These polyQ diseases share several clinical findings such as anticipation, somatic mosaicism (Tanaka et al., 1999), and selective neuronal and non-neuronal involvement despite widespread expression of the mutant gene (Zoghbi and Orr, 2000; Paulson, 2000). There is also an inverse correlation between the CAG repeat size and the age at onset, or the disease severity adjusted by the age at examination in SBMA (Doyu et al., 1992; La Spada et al., 1992; Igarashi et al., 1992) as well as other polyQ diseases (Duyao et al., 1993; Orr et al., 1993; Zoghbi and Orr, 2000; Paulson, 2000).

Previously, we reported nuclear inclusions (NIs) containing the mutant and truncated AR with expanded polyQ in the residual motor neurons in the brain stem and spinal cord (Li et al., 1998a) as well as in the skin, testis, and some other visceral organs of SBMA patients (Li et al., 1998b). The presence of NIs is a pathologic hallmark of most other polyQ diseases, and is considered to be relevant to pathophysiology (Zoghbi and Orr, 2000; Paulson, 2000). However, considerable controversy surrounds the importance of NIs in the pathophysiology of the polyQ diseases (Klement et al., 1998; Saudou et al., 1998; Cummings et al., 1999; Gutekunst et al., 1999). NIs may reflect a cellular mechanism that protects neurons from the toxic effects of polyQ tract, and nuclear translocation of the mutant protein may be essential in the pathophysiology of the majority of polyQ diseases. SBMA is unique among these disorders in that the mutant protein, AR, has a specific ligand, testosterone, and this ligand alters the subcellular localization of the protein by favoring its nuclear uptake. The AR is normally confined to a multi-heteromeric inactive complex in the cell cytoplasm, and translocates into the nucleus in a ligand-dependent manner (Zhou et al., 1994), which is likely enhanced in male SBMA patients. We took advantage of this ligand effect to study the role of nuclear uptake of the mutant protein on the disease manifestations in transgenic (Tg) mice.

Unlike the profound gender difference of phenotypes in SBMA patients, neither a Tg mouse model of SBMA expressing expanded pure 239 CAGs under the control of human AR promoter (Adachi et al., 2001) nor that carrying truncated *AR* with 112 CAGs (Abel et al., 2001) showed any remarkable phenotypic difference with gender. In the present study, we generated Tg mice with full-length *AR* containing 97 CAGs, showing neurologic phenotypes with significant sexual differences. Our findings reiterate the importance of nuclear localization of the mutant protein in the disease mechanism, and indicate an approach to effective treatment for SBMA.

Results

Tg Mice Carrying Full-Length Human *AR* with 97 CAGs Showed Sexual Differences in Symptoms, Transgene Expression, and Pathology

Symptomatic difference with gender: we generated Tg mice expressing the full-length human *AR* containing

[3]Correspondence: sobueg@med.nagoya-u.ac.jp
[4]These authors contributed equally to this work.

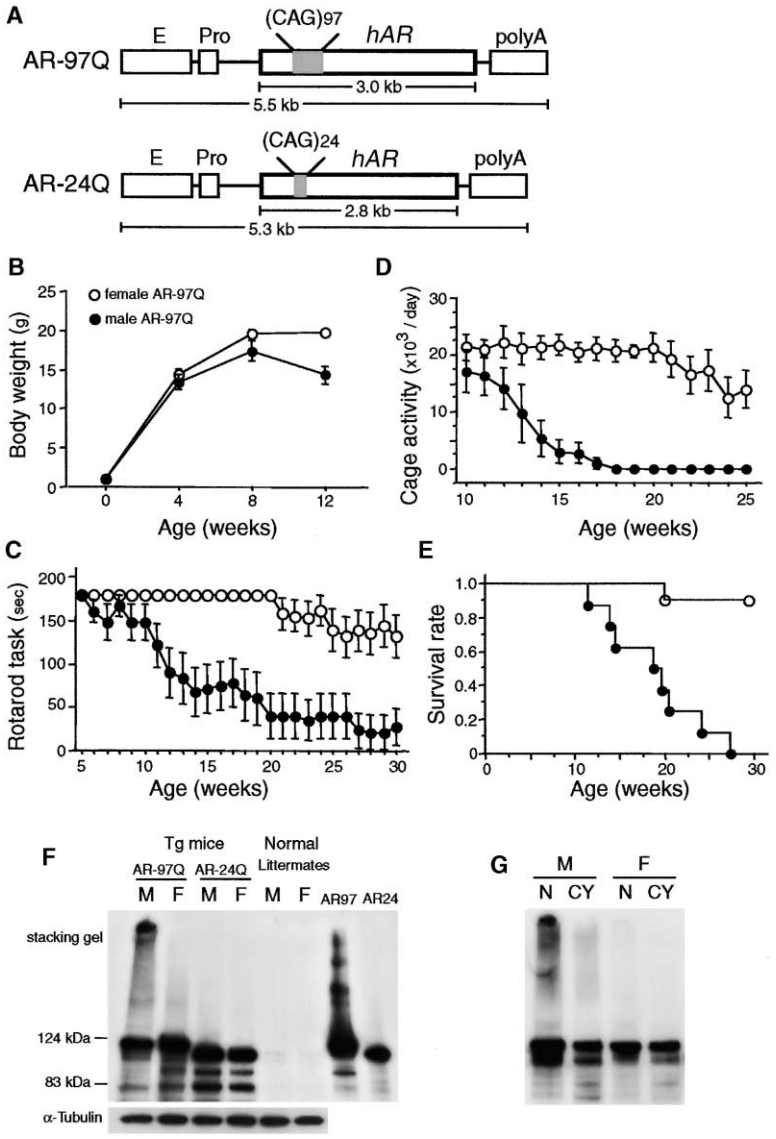

Figure 1. Sexual Differences in Symptomatic Phenotypes and Transgene Expression

(A) Schematic view of the transgene constructs. The microinjected fragment was composed of a cytomegalovirus enhancer (E), a chicken β-actin promoter (Pro), a full-length human *AR* containing 24 or 97 CAGs (*hAR*), and a rabbit β-globin polyadenylation signal sequence (polyA). (B, C, D, and E) Sexual differences in body weight (B, #2–6), rotarod task (C, #7–8), cage activity (D, #2–6), and survival rate (E, #7–8). All parameters are significantly different between the male AR-97Q mice (●, n = 8) and female AR-97Q mice (○, n = 8) ($p = 0.001$, $p = 0.003$, $p = 0.005$, and $p = 0.001$, respectively). (F) Western blot analysis of total homogenates from the muscle of the male (M) and female (F) mice of AR-97Q, AR-24Q, and normal littermates (12-week-old) immunolabeled by an antibody (N-20) against AR. Mouse AR was hardly detectable in the normal littermates. Comparison with muscle extracts from normal littermates indicated that most of the lower bands in transgenic (Tg) mice represent truncated human AR. Protein lysate from Neuro2a cells transfected with the transgene containing 24 CAGs and that with 97 CAGs (AR24 and AR97) are shown for size comparison. (G) Western blot analysis of nuclear (N) and cytoplasmic (CY) fractions from the muscle of the male (M) and female (F) AR-97Q mice (#7–8, 14-week-old) immunolabeled by N-20.

24 or 97 CAGs under the control of a cytomegalovirus enhancer and a chicken β-actin promoter (Figure 1A). We established 3 lines with 24 glutamines (AR-24Q) and 5 lines with 97 glutamines (AR-97Q). Copy numbers of the transgene were 1 to 5 in AR-24Q mice and 1 to 3 in AR-97Q mice (Table 1). We assessed the 24 or 97 CAG repeat in the transgene by the PCR amplification on the tail DNA using a fluorescently labeled primer, and subsequent size determination on the polyacrylamide gel did not show unequivocal intergenerational instability in the CAG repeat number (data not shown).

Three of five lines with AR-97Q (#2–6, #4–6, #7–8) exhibited progressive motor impairment, although no lines with AR-24Q showed any manifested phenotypes up to the latest age examined, 30 weeks old. All three symptomatic lines showed small body size, short life span, progressive muscle atrophy and weakness, as well as reduced cage activity, all of which were markedly pronounced and accelerated in the male AR-97Q mice, but not observed or far less severe in the female AR-97Q mice regardless of the line (Figures 1B–1E). The first detectable phenotype is muscle atrophy of the trunk and hindlimbs followed by weight loss and impairment of the rotarod task. We detected the onset of motor impairment by the rotarod task at 8 to 9 weeks of age in the male AR-97Q mice, while 15 weeks or more in the females (Table 1). The affected mice were hypoactive and dragged their hindlimbs. The forelimbs were not involved until hindlimb atrophy became severe. Males showed a markedly faster and earlier motor deficit than females, and shorter life span. The 50% mortality ranged from 66 to 132 days of age in the male AR-97Q mice of 3 lines, whereas mortality of the female AR-97Q mice remained only 10% to 30% at more than 210 days in the 3 lines. The cause of death was cachexia due to hyponutrition and dehydration.

Expression of transgene: Western blot analysis revealed the transgenic protein retained in the stacking gel as well as a single band of AR monomer consistent with 97 glutamines and truncated fragments of mutant

Table 1. Phenotypes of Transgenic Mice

Line	Copy Number	Onset of Weight Loss (Weeks)	Onset of Rotarod Impairment (Weeks)	Median Life Expectancy (Days)	1C2 Staining
AR-97Q					
2–6	1–3	6/16	9/18	66/>210	++/+
4–6	1–3	4/12	8/15	110/>210	++/+
7–8	1–3	8/16	9/21	132/>210	++/+
3–7	ND	8/−	−/−	>210	ND
8–5	ND	8/−	−/−	>210	ND
AR-24Q					
5–5	5	−/−	−/−	ND	−/−
8–7	1–3	−/−	−/−	ND	
12–13	1–3	−/−	−/−	ND	ND

Data is shown as male/female. −, not detected; +, detectable diffuse nuclear staining and nuclear inclusions; ++, abundant diffuse nuclear staining and nuclear inclusions; ND, not determined. All mice were examined until 30 weeks old.

AR in all symptomatic lines. We detected these proteins in the spinal cord, cerebrum, heart, muscle, and pancreas. Although the male AR-97Q mice had more protein within the stacking gel than the female AR-97Q mice, the female AR-97Q mice had more monomeric AR protein (Figure 1F). AR-24Q mice showed a single band of AR with 24 glutamines without protein in the stacking gel. The nuclear fraction contained the most transgene protein within the stacking gel (Figure 1G).

There was no significant difference in the expression of the mRNA of the transgene between the male and female AR-97Q mice (data not shown). These observations indicate that the nuclear localization is the major expression profile of the transgene protein in the stacking gel. This nuclear localization was more prominent in males than in females, while the mRNA expression levels were indistinguishable between genders.

Pathology: AR-24Q mice showed no pathologic abnormalities at the age of 12 weeks. In AR-97Q mice, we detected diffuse nuclear staining and less frequent NIs with 1C2, an antibody specifically recognizing the expanded polyQ (Trottier et al., 1995), in the neurons of the spinal cord, cerebrum, cerebellum, brain stem, and dorsal root ganglia as well as non-neuronal tissue such as the heart, muscle, and pancreas (Table 2). In the neuronal tissues, the nuclei of the motor neurons showed the most prominent diffuse nuclear staining and NIs. Glial cells also showed marked staining, but not the dorsal root ganglia. The regions with diffuse nuclear staining and NIs also showed immunoreactivity to an antibody to AR (N-20) (data not shown). Neither 1C2 nor N-20 revealed immunoreactivity in the cytoplasm. Diffuse nuclear staining and NIs were found at 4 weeks of age and became more profound with aging, although

Table 2. Distribution of Nuclear Inclusions and Diffuse Nuclear Staining with 1C2

Tissue	Male Nuclear Inclusions (NIs)/Diffuse Nuclear Staining (D)			Female Nuclear Inclusions (NIs)/Diffuse Nuclear Staining (D)		
Neuronal	Total NIs/D	Neuronal NIs/D	Glial NIs/D	Total NIs/D	Neuronal NIs/D	Glial NIs/D
Cerebral cortex	+/++	+/++	+/++	−∼+/+	−∼+/+	−∼+/+
Olfactory bulb	+∼++/++	+∼++/++	+/++	−∼+/+	−∼+/+	−∼+/+
Basal ganglia	+/++	+/++	+/++	−∼+/−∼+	−∼+/−∼+	−∼+/−∼+
Cerebellum	+∼++/++	+/++	+∼++/++	−∼+/+	−∼+/+	−∼+/+
Pons	+/++	+/++	+/++	−∼+/−∼+	−∼+/−∼+	−∼+/−∼+
Ependyma	−∼+/−∼+			−∼+/−∼+		
Spinal cord	++∼+++/+++	++/++∼+++	++/++∼+++	−∼+/+	−∼+/+	−∼+/+
Dosal root ganglia	−∼+/−∼+	−∼+/−∼+	−/−	−∼+/−∼+	−∼+/−∼+	−/−
Non-neuronal						
Muscle	++/+			−∼+/−∼+		
Heart	++/+			−∼+/−∼+		
Pancreas	−∼++/−∼++			−∼+/−∼+		
Eye	−∼+/−∼+			−/−		
Lung	−∼+/−∼+			−/−		
Kidney	−/−			−/−		
Liver	−/−			−/−		
Stomach	−/−			−/−		
Intestine	−/−			−/−		
Spleen	−/−			−/−		
Thymus	−/−			−/−		
Skin	−/−			−/−		
Prostate	−∼+					
Testis	−					
Ovary	−					

−, absent; + mild; ++, moderate; +++, abundant. In the case that the amount of NIs or D differs among three lines, we delineate its range. Three lines, #2–6, #4–6, and #7–8, were autopsied at 12, 18, 15 weeks of age, respectively.

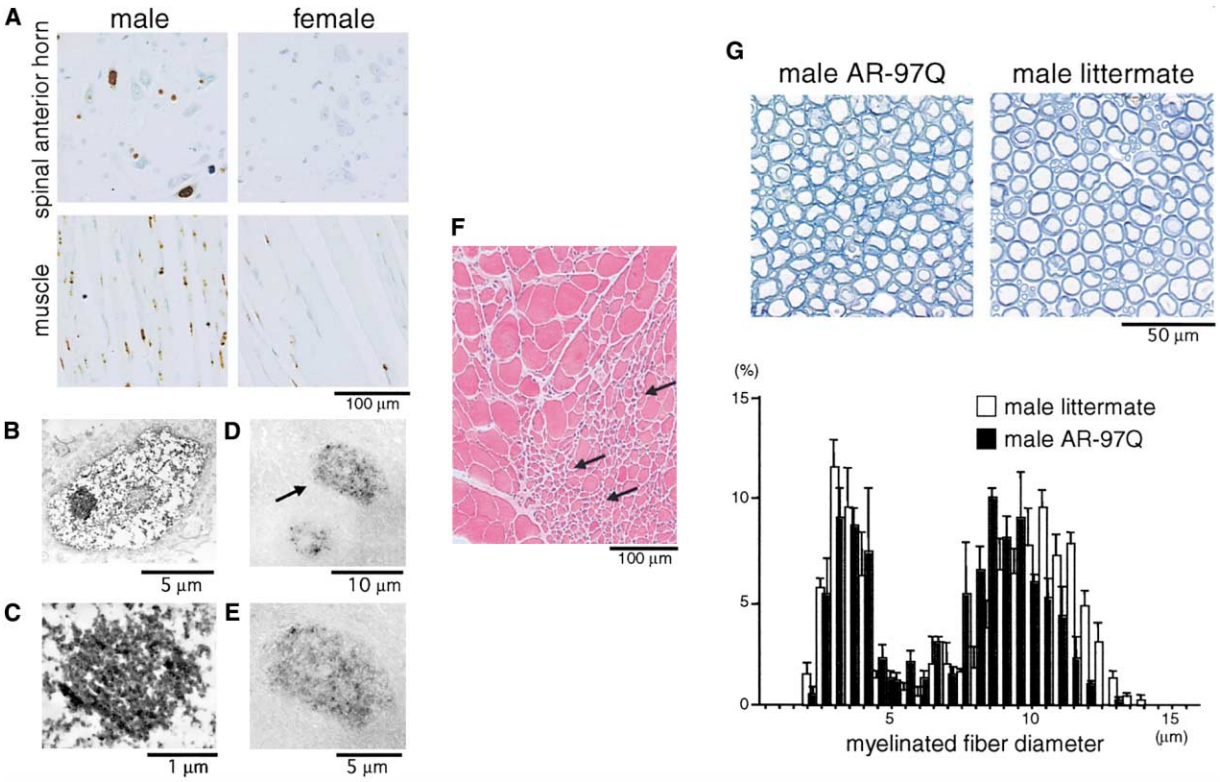

Figure 2. Pathologic Findings of AR-97Q Mice

(A) Immunohistochemical study of the spinal anterior horn and muscle of the male and female AR-97Q mice stained with a monoclonal antibody (1C2) against abnormally expanded polyglutamine (#7–8, 14-week-old). (B–E) Electron microscopic immunohistochemistry for 1C2 of an anterior horn cell (#4–6, 24-week-old). Dense granular aggregate of 1C2-immunoreactive material was recognized in the motor neuron nucleus which showed a nuclear inclusion in light micrograph (B, low magnification and C, high magnification). Another motor neuron (D, arrow), which demonstrated diffuse nuclear staining in light micrograph, showed microaggregates in high magnification (E). (F) HE staining of the muscle in the male AR-97Q mouse revealed obvious grouped atrophy and small angulated fibers (arrow) (#7–8, 14-week-old). (G) Toluidine blue staining and the histogram of myelinated fiber diameter of the L5 ventral root of male AR-97Q mice and their normal littermates. Large myelinated fibers in the ventral root showed axonal atrophy in the male AR-97Q mice (■, n = 3) compared with normal littermates (□, n = 3) (#7–8, 13-week-old).

male AR-97Q mice showed significantly more diffuse nuclear staining and NIs than females in agreement with the symptomatic and Western blot profile differences with gender (Table 2, Figure 2A). Electron microscopic immunohistochemistry for 1C2 demonstrated granular aggregates corresponding to NIs and fine microaggregates corresponding to diffuse nuclear staining in the neuronal tissues (Figures 2B–2E).

Muscle histology revealed significant grouped atrophy and small angulated fibers in the male AR-97Q mice as well as mild myopathic change such as increased variability in muscle fiber size (Figure 2F). Although the number of spinal motor neurons tended to be reduced in AR-97Q mice, the difference was not significant; 452 ± 10/10 sections in L5 segment of AR-97Q mice and 543 ± 28/10 sections in their littermates ($p = 0.10$). Nevertheless, the cross-sectional area of the individual spinal motor neurons significantly decreased in the male AR-97Q mice: 130.6 ± 4.0 μm^2 in L5 of male AR-97Q and 195.6 ± 12.1 μm^2 in their male littermates ($p = 0.006$). In addition, the diameter of large myelinated fibers (≥6.0 μm) was significantly diminished in the male AR-97Q mice (Figure 2G); the diameter of large fibers of the L5 ventral root was 8.49 ± 0.27 μm in male AR-97Q and 10.29 ± 1.08 μm in their male littermates ($p = 0.05$), whereas that of small fibers (<6.0 μm) was 3.11 ± 0.23 μm in male AR-97Q and 2.86 ± 0.11 μm in their male littermates ($p = 0.16$). Female AR-97Q mice showed no neuropathic changes. Neuronal cell population in the cerebrum, cerebellum, and dorsal root ganglia was fairly well preserved despite the abundant diffuse nuclear staining and NIs (data not shown).

Castration Prevents Phenotypic Expression in Male AR-97Q Mice

Castrated male AR-97Q mice showed marked improvement of symptoms, pathologic findings, and nuclear localization of the mutant AR compared with the sham-operated male AR-97Q mice. These castrated male AR-97Q mice weighed the same as their castrated male littermates, whereas the sham-operated male AR-97Q mice showed progressive emaciation (Figure 3A). Motor impairment assessed by rotarod and cage activity was significantly less or virtually absent in the castrated male AR-97Q mice as compared with the sham-operated male AR-97Q mice (Figures 3B and 3C). The castrated male AR-97Q mice showed motor impairment similar to that of the female AR-97Q mice. The life span was also

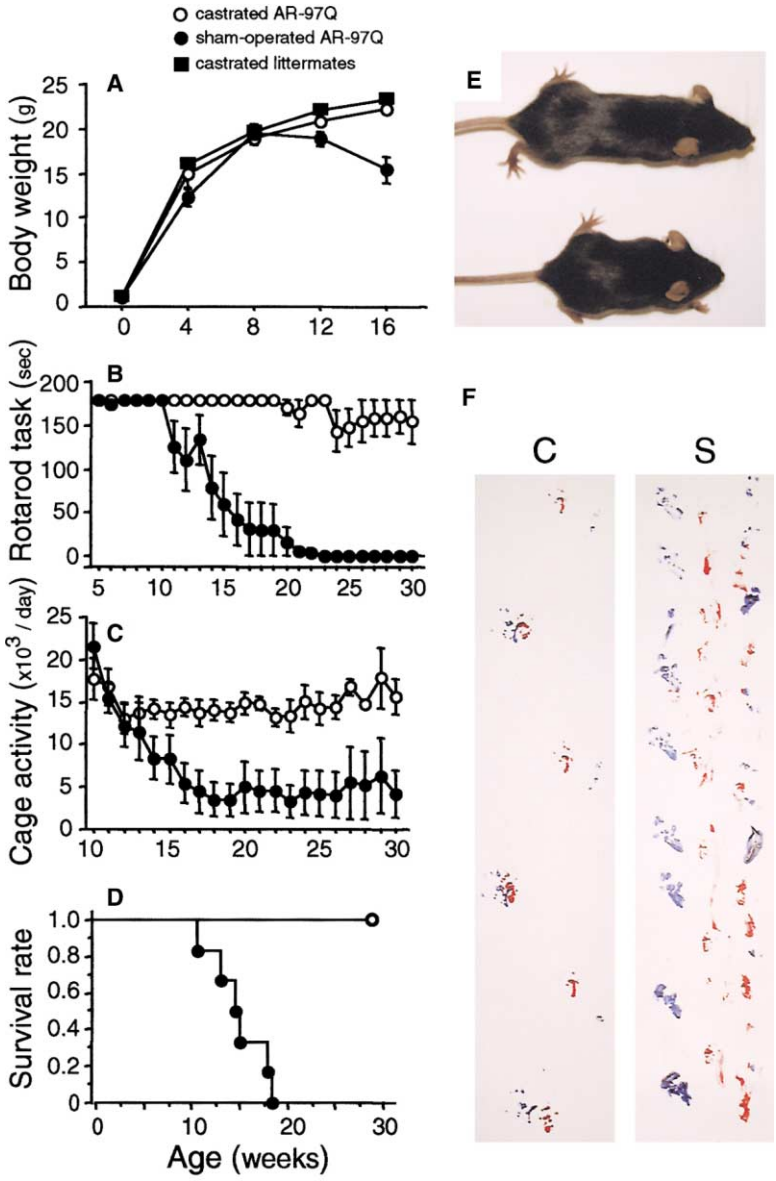

Figure 3. Effects of Castration on the Symptomatic Phenotypes of Male AR-97Q Mice

(A–D) Body weight (A, #7–8), rotarod task (B, #7–8), cage activity (C, #7–8), and survival rate (D, #2–6) of the castrated (○, n = 6) and sham-operated (●, n = 6) male AR-97Q mice. All parameters are significantly different between the sham-operated male AR-97Q mice and the castrated male AR-97Q mice or castrated male littermates (■, n = 2) ($p = 0.0001$, $p < 0.0001$, $p = 0.006$, and $p = 0.0006$, respectively). (E) The castrated AR-97Q mouse (top) shows no muscular atrophy, which is striking in the sham-operated male AR-97Q mouse (bottom) (#2–6, 12-week-old). (F) Footprints of 12-week-old castrated (C) and sham-operated (S) male AR-97Q mice (#2–6). Front paws are in red, and hind paws in blue paint.

significantly prolonged in the castrated male AR-97Q mice (Figure 3D). The castrated AR-97Q mice showed amelioration of muscle atrophy and body size reduction (Figure 3E). In a footprint analysis, the sham-operated male AR-97Q mice exhibited motor weakness with dragging of their hindlegs, which improved in the castrated male AR-97Q mice (Figure 3F). In the Western blot analysis using N-20, the mutant AR appearing within the stacking gel was markedly diminished in the castrated male AR-97Q mice compared with the sham-operated male AR-97Q mice (Figure 4A). The mutant AR in the nuclear fraction also significantly decreased in the castrated male AR-97Q mice (Figure 4B). The castrated male AR-97Q mice showed markedly diminished diffuse nuclear staining and NIs (Figure 4C). These observations suggested that castration markedly prevented nuclear localization of the mutant AR protein. The serum testosterone in the castrated male AR-97Q mice dramatically decreased to an undetectable low level, whereas that in sham-operated male AR-97Q mice was 27.7 ± 1.2 ng/dl (#7–8, n = 4).

Testosterone Administration Deteriorates Phenotypic Expression in Female Tg Mice

By contrast, testosterone administration markedly exacerbated symptoms, pathologic features, and nuclear localization of the mutant AR in the female AR-97Q mice. The testosterone-administered female AR-97Q mice showed progressive emaciation (Figure 5A). The motor impairment assessed by rotarod and cage activity was significantly worsened in the female AR-97Q mice administered testosterone, being similar to those of the untreated male AR-97Q mice (Figures 5B and 5C). The life span of the female AR-97Q mice was also affected by testosterone administration (Figure 5D). The testosterone-administered AR-97Q mice showed marked muscle atrophy and body size reduction (Figure 5E). In a footprint analysis, the testosterone-administered

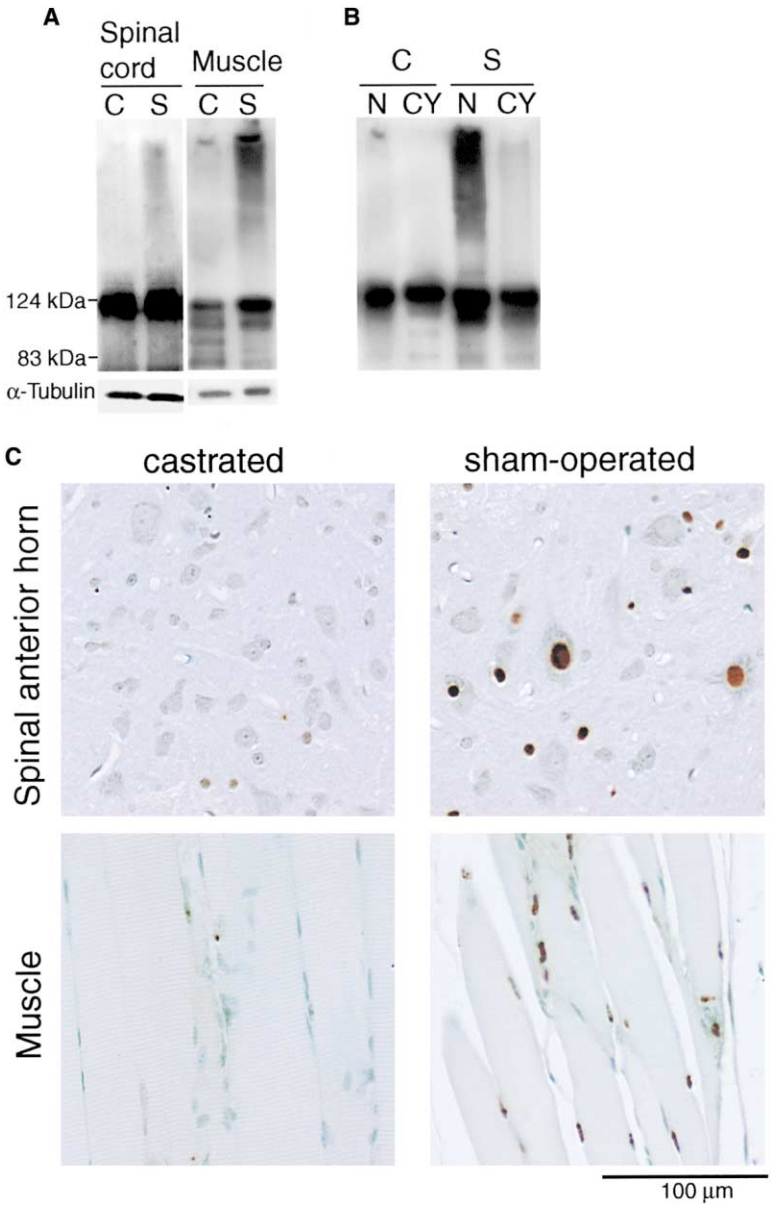

Figure 4. Effects of Castration on Transgene Expression and Neuropathology of Male AR-97Q Mice

(A) Western blot analysis of total homogenates from the spinal cord and muscle of the castrated (C) and sham-operated (S) male AR-97Q mice, which were immunolabeled by N-20 (#7–8, 13-week-old). (B) Western blot analysis of nuclear (N) and cytoplasmic (CY) fraction from the muscle of the castrated (C) and sham-operated (S) male AR-97Q mice, immunolabeled by N-20 (#7–8, 13-week-old). (C) Immunohistochemical study using 1C2 showed marked differences of diffuse nuclear staining and nuclear inclusions between the castrated and sham-operated AR-97Q mice in the spinal anterior horn and the muscle (#7–8, 13-week-old).

female AR-97Q mice exhibited motor weakness and dragged their hindlegs, which was not detected in the sesame oil-administered female AR-97Q mice (Figure 5F). Western blot analysis using N-20 revealed the mutant AR in the stacking gel in whole tissue homogenates as well as in the nuclear fraction, which was larger in amount in the testosterone-administered female AR-97Q mice than in the sesame oil-administered female AR-97Q mice (Figures 6A and 6B). The testosterone-administered female AR-97Q mice demonstrated markedly pronounced diffuse nuclear staining and NIs with 1C2 compared with the sesame oil-administered female AR-97Q mice (Figure 6C). The testosterone-administered female 97Q mice showed markedly higher serum testosterone levels (158.0 $\pm$ 70.7 ng/dl in #2–6, n = 3; 305.3 $\pm$ 182.3 ng/dl in #7–8, n = 4) than those in the sesame oil-administered female AR-97Q mice, all of which showed an undetectable low level.

Discussion

Our Tg mice with the full-length human *AR* containing 97 CAGs demonstrated progressive motor impairment and neuropathologic changes equivalent to human SBMA. Western blot analysis showed truncated fragments of mutant AR in the affected tissues. These fragments may contribute to pathophysiology in our Tg mice since several studies have suggested that proteolytic cleavage of mutant protein plays an important role in the pathogenic mechanisms of SBMA as well as other polyQ diseases (Li et al., 1998b; Kobayashi et al., 1998; Wellington et al., 1998; Mende-Mueller et al., 2001). Electron microscopic immunohistochemistry for 1C2 demonstrated granular aggregates and fine microaggregates, which indicates variable stages of pathologic change in the nucleus of motor neurons. Granular aggregate has also been reported in the pathologic study of

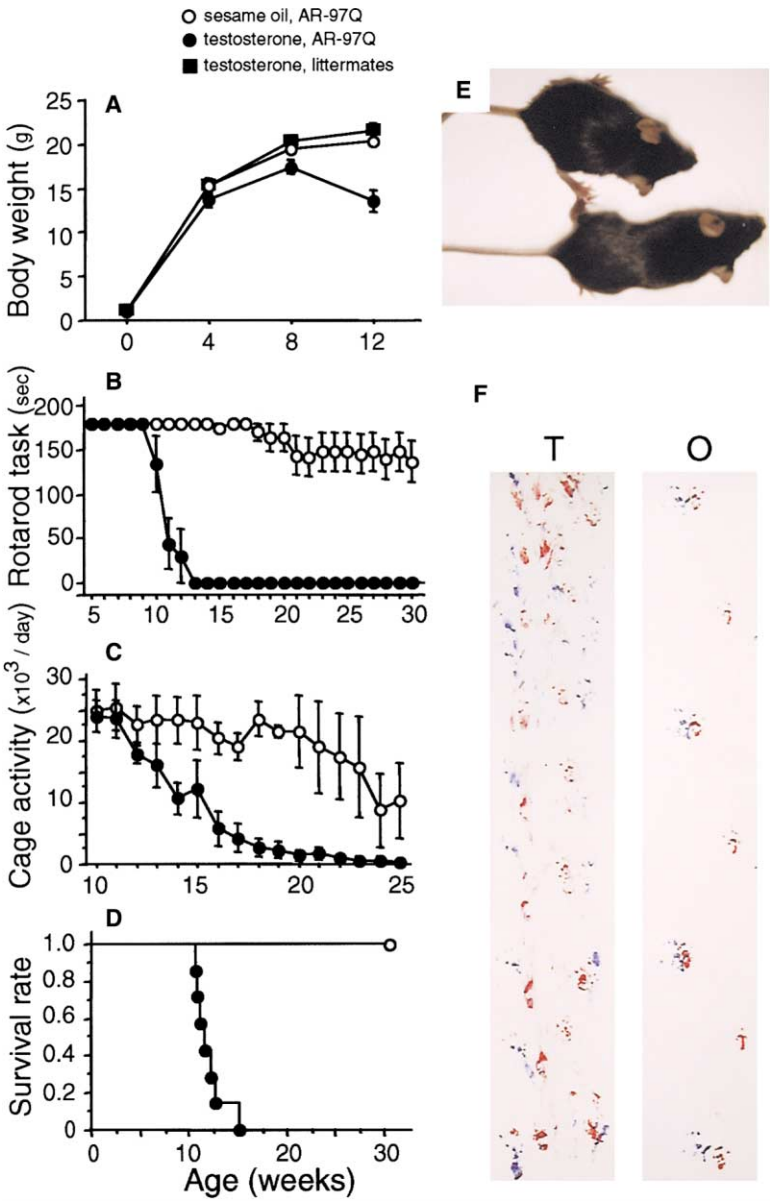

Figure 5. Effects of Testosterone Administration on the Symptomatic Phenotypes of Female AR-97Q Mice

(A–D) Body weight (A, #7–8), rotarod task (B, #7–8), cage activity (C, #2–6), and survival rate (D, #7–8) of the testosterone-administered (●, n = 7) and sesame oil-administered (○, n = 7) female AR-97Q mice. All parameters are significantly different between the testosterone-administered female AR-97Q mice and the sesame oil-administered female AR-97Q mice or testosterone-administered female littermates (■, n = 4) ($p < 0.0001$). (E) The testosterone-administered AR-97Q mouse (top) shows striking muscular atrophy, which is not demonstrated in the sesame oil-administered female AR-97Q mice (bottom) (#2–6, 14-week-old). (F) Footprints of 14-week-old testosterone-administered (T) and sesame oil-administered (O) female AR-97Q mice (#2–6).

SBMA (Li et al., 1998b). In our AR-97Q mice, neurogenic changes were evident in muscle pathology, and anterior horn cells and their axons showed significant decrease in size without substantial neuronal loss. These findings indicate that the main pathologic feature of our AR-97Q mice was neuronal dysfunction rather than degeneration of the spinal motor neurons, which was also demonstrated in a number of Tg mouse models of other polyQ diseases (Zoghbi and Orr, 2000; Rubinsztein, 2002). All symptomatic mice with AR-97Q showed motor impairment by 21 weeks of age; until this age, no lines with AR-24Q demonstrated rotarod deficit or weight loss in spite of the same expression levels of AR protein and similar copy numbers of the transgene. Nuclear inclusions and diffuse nuclear staining with 1C2 were found since 4 weeks of age even in female AR-97Q mice, although they are far less frequent than in male AR-97Q mice. Nevertheless, pathologic studies showed no abnormalities in AR-24Q mice at 12 weeks of age. These findings clarify that the symptomatic and pathologic phenotypes in AR-97Q were not due to overexpression of human AR but due to expanded polyglutamine tract. Moreover, no phenotypes were found in previous SBMA Tg mice with full-length human AR despite good transgene expression levels, presumably because the CAG repeat was not long enough (Bingham et al., 1995; La Spada et al., 1998).

Several Tg mouse models of SBMA have been reported so far. Since early models failed to manifest neurologic phenotypes (Bingham et al., 1995; La Spada et al., 1998; Merry et al., 1996), truncated AR and powerful promoter have been used in order to enhance phenotypes. A Tg mouse model of SBMA expressing expanded pure 239 CAGs under the control of human AR promoter (Adachi et al., 2001) and that carrying truncated *AR* with 112 CAGs controlled by prion protein

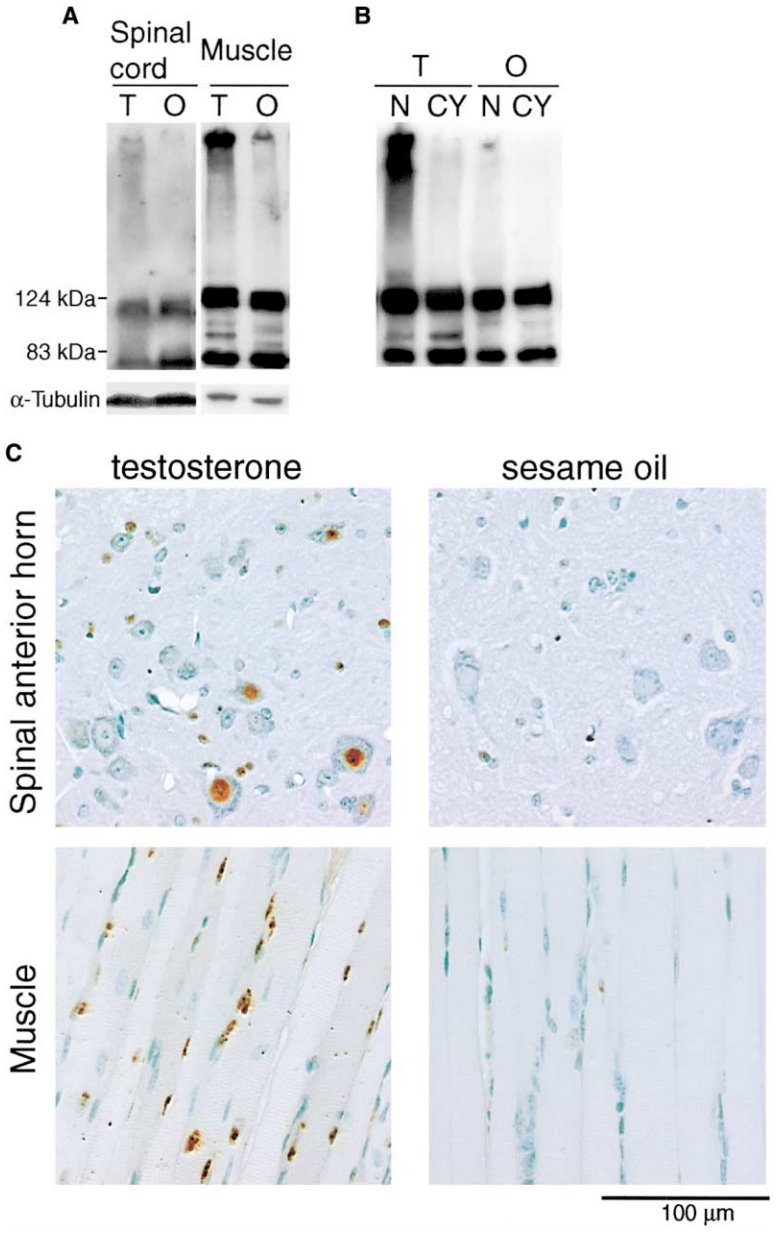

Figure 6. Effects of Testosterone Administration on Transgene Expression and Neuropathology of Female AR-97Q Mice

(A) Western blot analysis of total homogenates from the spinal cord and muscle of the testosterone-administered (T) and sesame oil-administered (O) female AR-97Q mice which were immunolabeled by N-20 (#2–6, 12-week-old). (B) Western blot analysis of nuclear (N) and cytoplasmic (CY) fraction from the muscle of the testosterone-administered (T) and sesame oil-administered (O) female AR-97Q mice, immunolabeled by N-20 (#2–6, 12-week-old). (C) Immunohistochemical study using 1C2 showed marked differences of diffuse nuclear staining and nuclear inclusions between the testosterone-administered and sesame oil-administered female AR-97Q mice in the spinal anterior horn and the muscle (#2–6, 12-week-old).

promoter (Abel et al., 2001) demonstrated progressive motor deficits and neuronal inclusions. They showed, however, no sexual difference of phenotypes because the transgenes of these Tg mice did not contain the ligand binding domain located in the C terminus of AR. Another Tg mouse model with the full-length AR showed motor impairment, although sexual difference of phenotypes has not been reported (Morrison et al., 2000).

The symptoms, pathologic findings, and nuclear localization of the mutant AR protein showed a remarkable sexual difference in our AR-97Q mice, and were significantly modified by hormonal intervention either by castration or testosterone administration. Although androgen has been shown to upregulate the expression of AR (Syms et al., 1985; Kemppainen et al., 1992; Zhou et al., 1995), RT-PCR did not reveal any significant sexual difference in the mRNA levels of the transgenic *AR* gene in our Tg mice, in which the transgene was not controlled by its own promoter with androgen-responsive element but by chicken β-actin promoter. These observations indicate that the testosterone level plays important roles in the sexual difference of phenotypes and effects of hormonal interventions, especially in the posttranscriptional stage of the mutant AR.

Castration dramatically prevented the phenotypic expression including neurologic findings in the male AR-97Q mice. The female AR-97Q mice, which showed few if any manifestations, demonstrated marked deterioration of symptoms by testosterone administration. The mutant AR located in the nuclei assessed by Western blot analysis and by immunohistochemistry with 1C2 dramatically diminished in the castrated male AR-97Q mice, and markedly increased in the testosterone-administered female AR-97Q mice. The castrated male AR-97Q

mice showed undetectable serum testosterone levels, whereas the testosterone-administered female AR-97Q mice showed markedly increased levels. Since the nuclear translocation of AR is solely dependent on testosterone (Stenoien et al., 1999; Simeoni et al., 2000), testosterone may show toxic effects in the female AR-97Q mice by accelerating nuclear translocation of the mutant AR. By contrast, castration prevented the nuclear localization of the mutant AR by reducing the testosterone level. The nuclear localization of the mutant protein with expanded polyQ is important in inducing neuronal cell dysfunction and degeneration in the majority of polyQ diseases. Addition of a nuclear export signal to the mutant huntingtin eliminates aggregate formation and cell death in cell models of HD (Saudou et al., 1998; Peters et al., 1999), and a nuclear localization signal had the opposite effect (Peters et al., 1999). In Tg mice of SCA1 having a mutated nuclear localization signal, ataxin-1 was distributed in the cytoplasm, and the mice did not show any neurologic disorders (Klement et al., 1998). These findings suggest that reduction of testosterone ameliorates phenotypic expression by preventing nuclear localization of the mutant AR. We emphasize that our approach, hormonal intervention to diminish testosterone level, can be applied to human therapy.

The castrated AR-97Q mice showed phenotypes similar to those of the female AR-97Q mice, implying that motor impairment of SBMA patients can be rescued to the level in female carriers. Almost half of the human SBMA female carriers showed mild subclinical electromyographic abnormalities, while few manifested clinical phenotypes (Sobue et al., 1993; Mariotti et al., 2000). Indeed, lower expression level of mutant AR in female carriers due to X inactivation may cause the escape from the manifestation, but our present study also suggests that the low level of testosterone prevents the nuclear localization of the expressed mutant AR, resulting in a lack of phenotypic manifestations in the female carriers.

A toxic gain of function has been considered the main stream of the pathophysiology in polyQ diseases, but a loss of function of mutant proteins may also play a role (Zoghbi and Orr, 2000; Rubinsztein, 2002). Although the expansion of polyQ tract in AR deteriorates the transcriptional activities of AR, and affects its interaction with other transcriptional factors and activators (Mhatre et al., 1993; Kazemi-Esfarjani et al., 1995; Chamberlain et al., 1994; Nakajima et al., 1996), the neurologic impairment in SBMA cannot be attributed to the loss of AR function (Maclean et al., 1995; McPhaul et al., 1993), a reason why testosterone shows insufficient and transient effects when used as a therapeutic agent for SBMA (Danek et al., 1994; Goldenberg and Bradley, 1996; Neuschmid-Kaspar et al., 1996). The present study further suggests that the major pathogenic mechanism of SBMA is a toxic gain of function of mutant AR with expanded polyQ, particularly when located in the nuclei. Although molecular mechanisms still remain to be elucidated, several studies have revealed that nuclear accumulation of the mutant protein resulted in sequestration of transcriptional regulatory proteins in SBMA and other polyQ diseases (McCampbell et al., 2000; Steffan et al., 2000; Nucifora et al., 2001).

There have been no substantially effective therapeutic approaches to the polyQ diseases. In a Tg mouse model of HD, expression of a dominant-negative caspase-1 mutant extended survival and delayed the appearance of neuronal inclusions, neurotransmitter receptor alterations, and onset of symptoms (Ona et al., 1999). Inhibition of mutant gene expression demonstrated the reversibility of phenotypic progression in a Tg mouse model of HD (Yamamoto et al., 2000). However, these gene modulations cannot be directly applied clinically. Transglutaminase inhibitors suppressed aggregate formation and apoptosis in a cell model of DRPLA (Igarashi et al., 1998) and prolonged survival in a Tg mouse model of HD (Karpuj et al., 2002). An in vitro model of HD showed inhibition of huntingtin fibrillogenesis by specific antibodies and small molecules (Heiser et al., 2000). Creatine increased survival and delayed motor symptoms in a Tg mouse model of HD (Andreassen et al., 2001). Overexpression of molecular chaperone HSP70 demonstrated preventive effects in a *Drosophila* model of Machado-Joseph disease (Warrick et al., 1999) and SCA1 cell and Tg mouse models (Cummings et al., 1998, 2001). HSP70 and HSP40 showed preventive effects also in an SBMA cell model (Kobayashi et al., 2000). These and other therapeutic approaches have, yet, remained insufficient or minimal in prevention of phenotypic expression and progression. Recently reported histone deacetylase inhibitors in a *Drosophila* model could be a promising candidate therapy for polyQ diseases (Steffan et al., 2001), but their therapeutic efficacy should be assessed in a Tg mouse model. Although no specific ligand of the mutant protein has been revealed in other polyQ diseases, the striking therapeutic effects of castration in our Tg mice further suggests that patients with polyQ disease can be rescued by prevention of the nuclear translocation of the mutant proteins. We emphasize that it is necessary to investigate hormone-like small molecules which alter the nuclear localization of mutant proteins for therapy of polyQ diseases.

Experimental Procedures

Transgene Construction

Chicken β-actin promoter-driven AR-24Q and AR-97Q constructs were prepared by digestion of pCAGGS vector (Niwa et al., 1991) by HindIII and ligation after filling in, which generated the new NheI site (pCAGGS-NheI). The full-length human *AR* fragment harboring 24 or 97 CAGs (Kobayashi et al., 1998) was subcloned into pCAGGS-NheI. By direct DNA sequencing, the presence of 24 and 97 CAG repeat sequences was confirmed in the 5.3 and 5.5 kb inserts, respectively.

Generation and Maintenance of Tg Mice and Genotyping

The final plasmids with SalI-NheI were digested to remove the *AR* fragments. We generated Tg mice by microinjection into BDF1 fertilized eggs, and obtained three founders with AR-24Q and five founders with AR-97Q. These mice were backcrossed to C57BL/6J. We screened mouse tail DNA by PCR for the presence of the transgene using the primers 5′-CTTCTGGCGTGTGACCGGCG -3′ and 5′-TGAGCTTGG CTGAATCTTCC-3′ and the confirmation of the CAG repeat size using the primers 5′-CCAGAGCGTGCGCGAAGTG-3′ and 5′-TGTGA AGGTTGCTGTTCCTC-3′. The transgene copy number in each line was determined by densitometric comparison of Southern blot hybridization intensity of the *AR* DNA with known standards cutting only one site in the transgene using SacII. For determining CAG repeat size, we electrophoresed the PCR products amplified with a Texas Red-labeled primer on 6% denaturing polyacrylamide gel for 12 hr using a 5500 DNA sequencer (Hitachi, Tokyo, Japan).

Neurological and Behavioral Testing

We analyzed rotarod task of mice by an Economex Rotarod (Columbus Instruments, Colombus, Ohio) weekly during the light phase of the 12 hr light/12 hr dark cycle as described previously (Adachi et al., 2001). We performed three trials, and recorded the longest duration on the rod for every mouse. We stopped the timer when the mouse fell from the rod or after an arbitrary limit of 180 s.

We measured cage activity while each mouse was in a transparent acrylic cage (16 × 30 × 14 cm, width × depth × height) housed in a soundproofed box. We used an AB system (Neuroscience, Tokyo, Japan) with an infrared ray sensor monitor to measure spontaneous motor activity. We automatically totaled and recorded all measurements for 24 hr per week at 10 min intervals.

Hormonal Intervention and Serum Testosterone Assay

Male AR-97Q mice and their normal littermates were castrated or sham-operated via the abdominal route under ketamine-xylazine anesthesia (50 mg/kg ketamine and 10 mg/kg xylazine, i.p.) at 4 weeks of age. Female AR-97Q mice and their littermates were subcutaneously injected 20 μg of testosterone enanthate dissolved in 20 μl of sesame oil weekly from 4 weeks of age until the end of the analysis. The sesame oil-administered mice were given the same amount of sesame oil.

We used Coat-A-Count Total Testosterone radioimmunoassay (Diagnostic Products Corporation, Los Angeles, California) for assaying the serum testosterone levels.

RNA and Protein Expression Analysis

We exsanguinated mice under ketamine-xylazine anesthesia, snap-froze their tissues with powdered CO_2 in acetone, extracted total RNA from tissues with Trizol (Life Technologies/Gibco BRL, Gaithersburg, Maryland), and reverse transcribed the RNA using SUPERSCRIPT II reverse transcriptase (Life Technologies/Gibco BRL). We used 5′-TTCCACACCCAGTGAAGC-3′ and 5′-GGCATTGGCCACAC CAAGCC-3′ as primers for specific transgene RNA detection. After amplification, the products were separated by agarose gel electrophoresis. We compared the intensity of the PCR products signals with those of β-actin mRNA levels, which were separately amplified, by ethidium bromide staining.

Frozen tissue (0.1 g wet weight) was homogenized in 1000 μl of 50 mM Tris (pH 8.0), 150 mM NaCl, 1% NP-40, 0.5% deoxycholate, 0.1% SDS, and 1 mM 2-mercaptoethanol with 1 mM PMSF and aprotinine at 6 μg/ml (2500 g for 15 min at 4°C). Each lane on a 5%–20% SDS-PAGE gel was loaded with protein 200 μg for nervous tissue, and 80 μg for muscular tissue from the supernatant fraction, which was transferred to Hybond-P membranes (Amersham Pharmacia Biotech, Buckinghamshire, England), using 25 mM Tris, 192 mM glycine, 0.1% SDS, and 10% methanol as transfer buffer. After immunoprobing with rabbit anti-AR antibody N-20 (1:1000) (Santa Cruz Biotechnology, Santa Cruz, California), we performed second antibody probing and detection using the ECL+plus kit (Amersham Pharmacia Biotech). Nuclear and cytoplasmic fractions were extracted with NE-PER nuclear and cytoplasmic extraction reagents (Pierce, Rockford, Illinois).

Immunohistochemistry

We perfused 20 ml of a 4% paraformaldehyde fixative in phosphate buffer (pH 7.4) through the left cardiac ventricle of mice deeply anesthetized with ketamine-xylazine, postfixed tissues overnight in 10% phosphate-buffered formalin, and processed tissues for paraffin embedding. Then we deparaffinized 4 μm thick tissue sections, dehydrated with alcohol, treated in formic acid for 5 min at room temperature, and stained with 1C2 (1:10000) (Chemicon, Temecula, California), as described before (Adachi et al., 2001).

For electron microscopic immunohistochemistry, we used paraffin-embedded tissue sections immunostained with 1C2 (1:10000) (Chemicon) as described previously (Adachi et al., 2001).

Muscle Histology and Morphometric Analysis of Spinal Motor Neurons and Ventral Spinal Roots

Six micrometer thick cryostat sections of the gastrocnemius muscles were air dried and stained with hematoxylin and eosin (H & E).

For assessment of the neuronal populations and cross-sectional area of the anterior horn cells, 20 serial 5 μm thick sections from the fifth lumbar spinal cords of three mice of each group (#7–8, 13-week-old) were prepared. Every other section was stained by the Nissl technique and all neurons with an obvious nucleolus, present in the anterior horn, were assessed using a Luzex FS image analyzer (Nireco, Tokyo, Japan) as described before (Terao et al., 1996). The diameter of myelinated fibers in the ventral spinal roots was measured on the transverse sections stained with toluidine blue as described before (Terao et al., 1996).

Statistical Analysis

We analyzed data using the unpaired t test and denoted p values of 0.05 or less as statistical significance.

Acknowledgments

We thank Dr. Jun-ichi Miyazaki for kindly providing pCAGGS vector, Dr. Masahiko Nishimura and Dr. Azumi Wada for instruction of castration, and Dr. Takashi Osada for preparation of testosterone. This work was supported by a Center-of-Excellence (COE) grant from the Ministry of Education, Culture, Sports, Science and Technology, Japan and grants from the Ministry of Health, Labor and Welfare, Japan.

Received: December 27, 2001
Revised: July 8, 2002

References

Abel, A., Walcott, J., Woods, J., Duda, J., and Merry, D.E. (2001). Expression of expanded repeat androgen receptor produces neurologic disease in transgenic mice. Hum. Mol. Genet. *10*, 107–116.

Adachi, H., Kume, A., Li, M., Nakagomi, Y., Niwa, H., Do, J., Sang, C., Kobayashi, Y., Doyu, M., and Sobue, G. (2001). Transgenic mice with an expanded CAG repeat controlled by the human AR promoter show polyglutamine nuclear inclusions and neuronal dysfunction without neuronal cell death. Hum. Mol. Genet. *10*, 1039–1048.

Andreassen, O.A., Dedeoglu, A., Ferrante, R.J., Jenkins, B.G., Ferrante, K.L., Thomas, M., Friedlich, A., Browne, S.E., Schilling, G., Borchelt, D.R., et al. (2001). Creatine increases survival and delays motor symptoms in a transgenic animal model of Huntington's disease. Neurobiol. Dis. *8*, 479–491.

Bingham, P.M., Scott, M.O., Wang, S., McPhaul, M.J., Wilson, E.M., Garbern, J.Y., Merry, D.E., and Fischbeck, K.H. (1995). Stability of an expanded trinucleotide repeat in the androgen receptor gene in transgenic mice. Nat. Genet. *9*, 191–196.

Chamberlain, N.L., Driver, E.D., and Miesfeld, R.L. (1994). The length and location of CAG trinucleotide repeats in the androgen receptor N-terminal domain affect transactivation function. Nucleic Acids Res. *22*, 3181–3186.

Cummings, C.J., Mancini, M.A., Antalffy, B., DeFranco, D.B., Orr, H.T., and Zoghbi, H.Y. (1998). Chaperone suppression of aggregation and altered subcellular proteasome localization imply protein misfolding in SCA1. Nat. Genet. *19*, 148–154.

Cummings, C.J., Reinstein, E., Sun, Y., Antalffy, B., Jiang, Y., Ciechanover, A., Orr, H.T., Beaudet, A.L., and Zoghbi, H.Y. (1999). Mutation of the E6-AP ubiquitin ligase reduces nuclear inclusion frequency while accelerating polyglutamine-induced pathology in SCA1 mice. Neuron *24*, 879–892.

Cummings, C.J., Sun, Y., Opal, P., Antalffy, B., Mestril, R., Orr, H.T., Dillmann, W.H., and Zoghbi, H.Y. (2001). Over-expression of inducible HSP70 chaperone suppresses neuropathology and improves motor function in SCA1 mice. Hum. Mol. Genet. *10*, 1511–1518.

Danek, A., Witt, T.N., Mann, K., Schweikert, H.U., Romalo, G., La Spada, A.R., and Fischbeck, K.H. (1994). Decrease in androgen binding and effect of androgen treatment in a case of X-linked bulbospinal neuronopathy. Clin. Investig. *72*, 892–897.

Duyao, M., Ambrose, C., Myers, R., Novelletto, A., Persichetti, F., Frontali, M., Folstein, S., Ross, C., Franz, M., Abbott, M., et al. (1993). Trinucleotide repeat length instability and age of onset in Huntington's disease. Nat. Genet. *4*, 387–392.

Doyu, M., Sobue, G., Mukai, E., Kachi, T., Yasuda, T., Mitsuma, T., and Takahashi, A. (1992). Severity of X-linked recessive bulbospinal neuronopathy correlates with size of the tandem CAG repeat in androgen receptor gene. Ann. Neurol. *32*, 707–710.

Goldenberg, J.N., and Bradley, W.G. (1996). Testosterone therapy and the pathogenesis of Kennedy's disease (X-linked bulbospinal muscular atrophy). J. Neurol. Sci. *135*, 158–161.

Gutekunst, C.A., Li, S.H., Yi, H., Mulroy, J.S., Kuemmerle, S., Jones, R., Rye, D., Ferrante, R.J., Hersch, S.M., and Li, X.J. (1999). Nuclear and neuropil aggregates in Huntington's disease: relationship to neuropathology. J. Neurosci. *19*, 2522–2534.

Heiser, V., Scherzinger, E., Boeddrich, A., Nordhoff, E., Lurz, R., Schugardt, N., Lehrach, H., and Wanker, E.E. (2000). Inhibition of huntingtin fibrillogenesis by specific antibodies and small molecules: implications for Huntington's disease therapy. Proc. Natl. Acad. Sci. USA *97*, 6739–6744.

Igarashi, S., Tanno, Y., Onodera, O., Yamazaki, M., Sato, S., Ishikawa, A., Miyatani, N., Nagashima, M., Ishikawa, Y., Sahashi, K., et al. (1992). Strong correlation between the number of CAG repeats in androgen receptor genes and the clinical onset of features of spinal and bulbar muscular atrophy. Neurology *42*, 2300–2302.

Igarashi, S., Koide, R., Shimohata, T., Yamada, M., Hayashi, Y., Takano, H., Date, H., Oyake, M., Sato, T., Sato, A., et al. (1998). Suppression of aggregate formation and apoptosis by transglutaminase inhibitors in cells expressing truncated DRPLA protein with an expanded polyglutamine stretch. Nat. Genet. *18*, 111–117.

Karpuj, M.V., Becher, M.W., Springer, J.E., Chabas, D., Youssef, S., Pedotti, R., Mitchell, D., and Steinman, L. (2002). Prolonged survival and decreased abnormal movements in transgenic model of Huntington disease, with administration of the transglutaminase inhibitor cystamine. Nat. Med. *8*, 143–149.

Kazemi-Esfarjani, P., Trifiro, M.A., and Pinsky, L. (1995). Evidence for a repressive function of the long polyglutamine tract in the human androgen receptor: possible pathogenetic relevance for the (CAG)n-expanded neuronopathies. Hum. Mol. Genet. *4*, 523–527.

Kemppainen, J.A., Lane, M.V., Sar, M., and Wilson, E.M. (1992). Androgen receptor phosphorylation, turnover, nuclear transport and transcriptional activation. J. Biol. Chem. *267*, 968–974.

Kennedy, W.R., Alter, M., and Sung, J.H. (1968). Progressive proximal spinal and bulbar muscular atrophy of late onset. A sex-linked recessive trait. Neurology *18*, 671–680.

Klement, I.A., Skinner, P.J., Kaytor, M.D., Yi, H., Hersch, S.M., Clark, H.B., Zoghbi, H.Y., and Orr, H.T. (1998). Ataxin-1 nuclear localization and aggregation: role in polyglutamine-induced disease in SCA1 transgenic mice. Cell *95*, 41–53.

Kobayashi, Y., Miwa, S., Merry, D.E., Kume, A., Mei, L., Doyu, M., and Sobue, G. (1998). Caspase-3 cleaves the expanded androgen receptor protein of spinal and bulbar muscular atrophy in a polyglutamine repeat length-dependent manner. Biochem. Biophys. Res. Commun. *252*, 145–150.

Kobayashi, Y., Kume, A., Li, M., Doyu, M., Hata, M., Ohtsuka, K., and Sobue, G. (2000). Chaperones Hsp70 and Hsp40 suppress aggregate formation and apoptosis in cultured neuronal cells expressing truncated androgen receptor protein with expanded polyglutamine tract. J. Biol. Chem. *275*, 8772–8778.

La Spada, A.R., Wilson, E.M., Lubahn, D.B., Harding, A.E., and Fischbeck, K.H. (1991). Androgen receptor gene mutations in X-linked spinal and bulbar muscular atrophy. Nature *352*, 77–79.

La Spada, A.R., Roling, D.B., Harding, A.E., Warner, C.L., Spiegel, R., Hausmanowa-Petrusewicz, I., Yee, W.C., and Fischbeck, K.H. (1992). Meiotic stability and genotype-phenotype correlation of the trinucleotide repeat in X-linked spinal and bulbar muscular atrophy. Nat. Genet. *2*, 301–304.

La Spada, A.R., Peterson, K.R., Meadows, S.A., McClain, M.E., Jeng, G., Chmelar, R.S., Haugen, H.A., Chen, K., Singer, M.J., Moore, D., et al. (1998). Androgen receptor YAC transgenic mice carrying CAG 45 alleles show trinucleotide repeat instability. Hum. Mol. Genet. *7*, 959–967.

Li, M., Miwa, S., Kobayashi, Y., Merry, D.E., Yamamoto, M., Tanaka, F., Doyu, M., Hashizume, Y., Fischbeck, K.H., and Sobue, G. (1998a). Nuclear inclusions of the androgen receptor protein in spinal and bulbar muscular atrophy. Ann. Neurol. *44*, 249–254.

Li, M., Nakagomi, Y., Kobayashi, Y., Merry, D.E., Tanaka, F., Doyu, M., Mitsuma, T., Hashizume, Y., Fischbeck, K.H., and Sobue, G. (1998b). Nonneural nuclear inclusions of androgen receptor protein in spinal and bulbar muscular atrophy. Am. J. Pathol. *153*, 695–701.

MacLean, H.E., Warne, G.L., and Zajac, J.D. (1995). Defects of androgen receptor function: from sex reversal to motor neurone disease. Mol. Cell. Endocrinol. *112*, 133–141.

Mariotti, C., Castellotti, B., Pareyson, D., Testa, D., Eoli, M., Antozzi, C., Silani, V., Marconi, R., Tezzon, F., Siciliano, G., et al. (2000). Phenotypic manifestations associated with CAG-repeat expansion in the androgen receptor gene in male patients and heterozygous females: a clinical and molecular study of 30 families. Neuromuscul. Disord. *10*, 391–397.

McCampbell, A., Taylor, J.P., Taye, A.A., Robitschek, J., Li, M., Walcott, J., Merry, D., Chai, Y., Paulson, H., Sobue, G., and Fischbeck, K.H. (2000). CREB-binding protein sequestration by expanded polyglutamine. Hum. Mol. Genet. *9*, 2197–2202.

McPhaul, M.J., Marcelli, M., Zoppi, S., Griffin, J.E., and Wilson, J.D. (1993). Genetic basis of endocrine disease. 4. The spectrum of mutations in the androgen receptor gene that causes androgen resistance. J. Clin. Endocrinol. Metab. *76*, 17–23.

Mende-Mueller, L.M., Toneff, T., Hwang, S.R., Chesselet, M.F., and Hook, V.Y. (2001). Tissue-specific proteolysis of Huntingtin (htt) in human brain: evidence of enhanced levels of N- and C-terminal htt fragments in Huntington's disease striatum. J. Neurosci. *21*, 1830–1837.

Merry, D.E., McCampbell, A., Taye, A.A., Winston, R.L., and Fischbeck, K.H. (1996). Toward a mouse model for spinal and bulbar muscular atrophy: effect of neuronal expression of androgen receptor in transgenic mice. Am. J. Hum. Genet. Suppl. *59*, A271.

Mhatre, A.N., Trifiro, M.A., Kaufman, M., Kazemi-Esfarjani, P., Figlewicz, D., Rouleau, G., and Pinsky, L. (1993). Reduced transcriptional regulatory competence of the androgen receptor in X-linked spinal and bulbar muscular atrophy. Nat. Genet. *5*, 184–188.

Morrison, J.P., McManamny, P., O'Bryan, K.M., Cimdins, K.L., Kola, I., Cheema, S., and deKretser, D.M. (2000). A mouse model of spinal bulbar muscular atrophy (SBMA). Am. J. Hum. Genet. Suppl. 67, A51.

Nakajima, H., Kimura, F., Nakagawa, T., Furutama, D., Shinoda, K., Shimizu, A., and Ohsawa, N. (1996). Transcriptional activation by the androgen receptor in X-linked spinal and bulbar muscular atrophy. J. Neurol. Sci. *142*, 12–16.

Neuschmid-Kaspar, F., Gast, A., Peterziel, H., Schneikert, J., Muigg, A., Ransmayr, G., Klocker, H., Bartsch, G., and Cato, A.C. (1996). CAG-repeat expansion in androgen receptor in Kennedy's disease is not a loss of function mutation. Mol. Cell. Endocrinol. *117*, 149–156.

Niwa, H., Yamamura, K., and Miyazaki, J. (1991). Efficient selection for high-expression transfectants with a novel eukaryotic vector. Gene *108*, 193–199.

Nucifora, F.C., Jr., Sasaki, M., Peters, M.F., Huang, H., Cooper, J.K., Yamada, M., Takahashi, H., Tsuji, S., Troncoso, J., Dawson, V.L., et al. (2001). Interference by huntingtin and atrophin-1 with CBP-mediated transcription leading to cellular toxicity. Science *291*, 2423–2428.

Ona, V.O., Li, M., Vonsattel, J.P., Andrews, L.J., Khan, S.Q., Chung, W.M., Frey, A.S., Menon, A.S., Li, X.J., Stieg, P.E., et al. (1999). Inhibition of caspase-1 slows disease progression in a mouse model of Huntington's disease. Nature *399*, 263–267.

Orr, H.T., Chung, M.Y., Banfi, S., Kwiatkowski, T.J., Jr., Servadio, A., Beaudet, A.L., McCall, A.E., Duvick, L.A., Ranum, L.P., and Zoghbi, H.Y. (1993). Expansion of an unstable trinucleotide CAG repeat in spinocerebellar ataxia type 1. Nat. Genet. *4*, 221–226.

Paulson, H.L. (2000). Toward an understanding of polyglutamine neurodegeneration. Brain Pathol. *10*, 293–299.

Peters, M.F., Nucifora, F.C., Jr., Kushi, J., Seaman, H.C., Cooper, J.K., Herring, W.J., Dawson, V.L., Dawson, T.M., and Ross, C.A.

(1999). Nuclear targeting of mutant Huntingtin increases toxicity. Mol. Cell. Neurosci. *14*, 121–128.

Rubinsztein, D.C. (2002). Lessons from animal models of Huntington's disease. Trends Genet. *18*, 202–209.

Saudou, F., Finkbeiner, S., Devys, D., and Greenberg, M.E. (1998). Huntingtin acts in the nucleus to induce apoptosis but death does not correlate with the formation of intranuclear inclusions. Cell *95*, 55–66.

Simeoni, S., Mancini, M.A., Stenoien, D.L., Marcelli, M., Weigel, N.L., Zanisi, M., Martini, L., and Poletti, A. (2000). Motoneuronal cell death is not correlated with aggregate formation of androgen receptors containing an elongated polyglutamine tract. Hum. Mol. Genet. *9*, 133–144.

Sobue, G., Hashizume, Y., Mukai, E., Hirayama, M., Mitsuma, T., and Takahashi, A. (1989). X-linked recessive bulbospinal neuronopathy. A clinicopathological study. Brain *112*, 209–232.

Sobue, G., Doyu, M., Kachi, T., Yasuda, T., Mukai, E., Kumagai, T., and Mitsuma, T. (1993). Subclinical phenotypic expressions in heterozygous females of X-linked recessive bulbospinal neuronopathy. J. Neurol. Sci. *117*, 74–78.

Steffan, J.S., Kazantsev, A., Spasic-Boskovic, O., Greenwald, M., Zhu, Y.Z., Gohler, H., Wanker, E.E., Bates, G.P., Housman, D.E., and Thompson, L.M. (2000). The Huntington's disease protein interacts with p53 and CREB-binding protein and represses transcription. Proc. Natl. Acad. Sci. USA *97*, 6763–6768.

Steffan, J.S., Bodai, L., Pallos, J., Poelman, M., McCampbell, A., Apostol, B.L., Kazantsev, A., Schmidt, E., Zhu, Y.Z., Greenwald, M., et al. (2001). Histone deacetylase inhibitors arrest polyglutamine-dependent neurodegeneration in Drosophila. Nature *413*, 739–743.

Stenoien, D.L., Cummings, C.J., Adams, H.P., Mancini, M.G., Patel, K., DeMartino, G.N., Marcelli, M., Weigel, N.L., and Mancini, M.A. (1999). Polyglutamine-expanded androgen receptors form aggregates that sequester heat shock proteins, proteasome components and SRC-1, and are suppressed by the HDJ-2 chaperone. Hum. Mol. Genet. *8*, 731–741.

Syms, A.J., Norris, J.S., Panko, W.B., and Smith, R.G. (1985). Mechanism of androgen-receptor augmentation: analysis of receptor synthesis and degradation by the density-shift technique. J. Biol. Chem. *260*, 455–461.

Tanaka, F., Reeves, M.F., Ito, Y., Matsumoto, M., Li, M., Miwa, S., Inukai, A., Yamamoto, M., Doyu, M., Yoshida, M., et al. (1999). Tissue-specific somatic mosaicism in spinal and bulbar muscular atrophy is dependent on CAG-repeat length and androgen receptor-gene expression level. Am. J. Hum. Genet. *65*, 966–973.

Terao, S., Sobue, G., Hashizume, Y., Li, M., Inagaki, T., and Mitsuma, T. (1996). Age-related changes in human spinal ventral horn cells with special reference to the loss of small neurons in the intermediate zone: a quantitative analysis. Acta Neuropathol. (Berl.) *92*, 109–114.

Trottier, Y., Lutz, Y., Stevanin, G., Imbert, G., Devys, D., Cancel, G., Saudou, F., Weber, C., David, G., Tora, L., et al. (1995). Polyglutamine expansion as a pathological epitope in Huntington's disease and four dominant cerebellar ataxias. Nature *378*, 403–406.

Warrick, J.M., Chan, H.Y., Gray-Board, G.L., Chai, Y., Paulson, H.L., and Bonini, N.M. (1999). Suppression of polyglutamine-mediated neurodegeneration in Drosophila by the molecular chaperone HSP70. Nat. Genet. *23*, 425–428.

Wellington, C.L., Ellerby, L.M., Hackam, A.S., Margolis, R.L., Trifiro, M.A., Singaraja, R., McCutcheon, K., Salvesen, G.S., Propp, S.S., Bromm, M., et al. (1998). Caspase cleavage of gene products associated with triplet expansion disorders generates truncated fragments containing the polyglutamine tract. J. Biol. Chem. *273*, 9158–9167.

Yamamoto, A., Lucas, J.J., and Hen, R. (2000). Reversal of neuropathology and motor dysfunction in a conditional model of Huntington's disease. Cell *101*, 57–66.

Zhou, Z.X., Wong, C.I., Sar, M., and Wilson, E.M. (1994). The androgen receptor: an overview. Recent Prog. Horm. Res. *49*, 249–274.

Zhou, Z.X., Lane, M.V., Kemppainen, J.A., French, F.S., and Wilson, E.M. (1995). Specificity of ligand-dependent androgen receptor stabilization: receptor domain interactions influence ligand dissociation and receptor stability. Mol. Endocrinol. *9*, 208–218.

Zoghbi, H.Y., and Orr, H.T. (2000). Glutamine repeats and neurodegeneration. Annu. Rev. Neurosci. *23*, 217–247.